Materials Research. 2018; 21(4): e20180057
DOI: http://dx.doi.org/10.1590/1980-5373-MR-2018-0057

Solution Treatment Behaviors of 6061 Aluminum Alloy Prepared by Powder Thixoforming

Xuezheng Zhang*[a], *Tijun Chen*[a]

[a]*State Key Laboratory of Advanced Processing and Recycling of Nonferrous Metals, Lanzhou University of Technology, Lanzhou 730050, China*

Received: January 23, 2018; Accepted: March 26, 2018

Powder thixoforming (PTF) was a promising processing technology that can be used to fabricate high strength particle reinforced aluminum matrix composites, and a pioneer 6061 matrix alloy was fabricated utilizing PTF to investigate its solution treatment behaviors. A comparison study with traditional permanent mold cast (PMC) 6061 alloy disclosed that PTF alloy showed significantly reduced pore amount with only 0.16% (3.50% for PMC alloy). During solution treatment, PTF alloy displayed a much quicker solutionization progress than PMC alloy because of coarse eutectic phases and primary dendrites in latter alloy, its peak values of 14.5%, 241 MPa and 195 MPa in elongation, ultimate tensile strength and yield strength were achieved at 560ºC, an enhancement of 81.3%, 33.9% and 97.0%, respectively, compared with as-fabricated alloy. The dissolution of eutectic phases plays a dominative role in the growth of the primary α phases and secondarily primary α phases within 535ºC. However, the coarsening after 535ºC is subject to a mixture model involving atom diffusion along grain boundaries and through the crystal lattice. The superior tensile strengths of PTF alloy than PMC alloy resulted from decreased grain size, enhanced solid solution strengthening, reduced porosities and decreased harmful effect of insoluble phases in PTF alloy.

Keywords: *solution treatment, powder thixoforming, microstructure, tensile properties.*

1. Introduction

Aluminum matrix composites (AMCs) reinforced with particulates have a combination of superior properties, e.g., light weight, high stiffness, high wear resistance and high specific strength. Numerous methods have been utilized to manufacture particle reinforced AMCs, for instance, diffusion bonding[1,2], compo-casting[3,4] and powder metallurgy[5,6]. Powder metallurgy is especially applicable because its processing temperature is relatively low and particle reinforcements can be uniformly dispersed. However, the as-fabricated composites inevitably contain certain amounts of voids although advanced sintering techniques are utilized[5]. Besides, increasing difficulties are encountered in the fabrication of components with complex shape or large size. Considering that thixoforming is able to significantly decrease voids and manufacture shape-complicated as well as large-sized components, a promising technology named powder thixoforming (PTF) was proposed by combining powder metallurgy with thixoforming. Its preparation procedure is generally as follows. At first, the blending and pressing processes of powder metallurgy are employed to obtain a green composite ingot. Subsequently, the green ingot is subjected to partial remelting so as to acquire a non-dendritic semisolid ingot. The semisolid ingot is ultimately thixoformed prior to the fabrication of a composite component. A decreased amount of porosities as well as a uniform dispersion of particulate reinforcements in the composite can be achieved by utilizing this method. In addition, PTF has a lower potential cost than powder metallurgy.

As one of the most widely used AMCs matrix alloys, 6061 aluminum alloy is heat-treatable and its mechanical properties depend strongly upon heat treatment. Researches have disclosed that the mechanical properties of AMCs, especially these reinforced by particulates, can also be enhanced via heat treatment[7-9]. The enhanced matrix yield strength provides more efficient load transfer from the matrix to the particulate reinforcement. So far, most of available researches related to the heat treatment behaviors of particulate reinforced AMCs are mainly focused on these produced by powder metallurgy[10,11], hot extrusion[12] as well as permanent mold casting[13]. However, the optimum heat treatment parameters for composites prepared by these conventional techniques are not applicable to PTF because of the huge differences in the microstructure of the resultant composites. In addition to the high cost of composite materials, it is vital to optimize heat treatment parameters for PTF technique to maximize the mechanical properties of the produced composites. And the influences of heat treatment on the matrix alloy need to be verified in advance in effort to have a better understanding of its influence on corresponding AMCs. Unfortunately, only a

*e-mail: chentj@lut.cn

few works to date involved the heat treatment behaviors of PTF materials[14-16]. A preliminary investigation on the solution time has shown a remarkable improvement in the tensile properties of the PTF-6061 alloy after being solutionized at 535ºC for 3 h[14]. However, the influence of solution temperature on the tensile properties has demonstrated to be larger than that of solution time because of the accelerated diffusion rate of solute atoms[17,18]. It is therefore believed that an investigation of the influences of solution temperature on the microstructure and tensile properties of the PTF-6061 alloy would be appropriate. Besides, as an extension of the previous study (i.e., Ref.[14]), this work would greatly facilitate the systematic understanding on the solution treatment behaviors of PTF materials. In this paper, a comparison study with permanent mold cast (PMC) 6061 alloy that had been widely investigated was conducted in order to elucidate the characteristics of PTF technique during solution treatment.

2. Materials and Methods

2.1 Materials preparation

The raw material used in the fabrication of the PTF alloy was atomized 6061 alloy powders having a mean diameter of about 17.91 μm and its nominal composition was presented in Table 1. The fabrication procedure was as follows. Firstly, the 6061 alloy powders were cold pressed into a sample with diameter of 50 mm and thickness of 15 mm and subsequently it was heated in a resistance furnace at a semisolid temperature of 660ºC for 80 min in accordance with a preliminary study[19]. The heated specimen was rapidly placed into a forging mold and ultimately thixoforged under a pressure of 160 MPa. Repeating the aforementioned steps, certain PTF-6061 alloy samples were prepared. In attempt to elucidate the feature of PTF technique, the material of PMC-6061 alloy was also produced for the purpose of comparison. The PMC-6061 alloy was prepared through pure Al, Mg, Cu, and an Al-20 wt% Si master alloy, and a resulting composition of Al-1.0Mg-0.6Si-0.3Cu (wt%) were achieved. The fabrication process is as follows. To begin with, a resistance furnace with a pre-set temperature of 750 °C was used to melt a certain amount of the pure metals and master alloy. Then 1.5% (mass fraction) C_2Cl_6 was added into the melt at 730 °C for degassing. Subsequently, the melt was held for 5 min before it was poured into a permanent mold with length of 500 mm and diameter of 50 mm. Some cake specimens with dimensions of Ø50×15 mm were cut from the cast rods.

2.2 Solution treatment

A preliminary investigation revealed that the PTF-6061 and PMC-6061 alloys achieved the best comprehensive mechanical properties after being solutionized at 535ºC for 3 and 6 h, respectively[14]. Therefore, the respective solution times of 3 and 6 h for the PTF alloy and the PMC alloy were employed in this paper so as to get the optimal solution temperature. A resistance furnace was used to solutionize the two kinds of cake samples with the same dimensions at the temperatures of 485ºC, 510ºC, 535ºC, 560ºC and 585ºC[20] prior to rapid water quenching.

2.3 Material characterization

Standard preparation procedure was utilized to obtain the metallographic specimens[15]. The characterization of alloy microstructure was implemented on a QUANTA FEG 450 scanning electron microscope (SEM) equipped with an energy dispersive spectroscope (EDS) and on an MeF3 optical microscope (OM). Image-Pro Plus 6.0 software was used to examine the alloy grain size through randomly captured OM images with a magnification of 500×, and the mean values for each alloy were determined by at least ten images. The Archimedes method was used to measure the density of the samples in an attempt to evaluate the porosity percentage of the samples. In order to examine the tensile performance of these two kinds of alloys, tensile testing was conducted at room temperature and the experimental details can be found elsewhere[16]. At last, the fracture surface of the samples was observed on the SEM and the side views of the fracture surface were detected on the OM. Electron probe microanalyzer (EPMA-1600) was utilized to determine the fractional concentration of solute elements in the α-Al phases during solution treatment, which was based on the average of five values.

3. Results and Discussion

3.1 Porosity evaluation

In an attempt to verify the effectiveness of PTF in decreasing porosities as mentioned above, the as-obtained microstructures of these two materials were firstly examined. Fig.1 displays the representative SEM images of porosity distribution in these two kinds of alloys under the same magnification. As shown in Fig.1a, few pores can be found in the PTF alloy and statistical results suggested that the porosity percentage of the PTF alloy was only 0.16%.

Table 1. Nominal composition of 6061 aluminum alloy employed in this work.

Mg	Si	Cu	Fe	Zn	Cr	Ti	Al
0.8%−1.2%	0.4%−0.8%	0.15%−0.4%	0.7%	0.25%	0.04%−0.35%	0.15%	Balance

For reference, the pore amount in the PMC alloy was also measured (Fig.1b) and its quantity was up to 3.50%. This distinct reduction in the porosity of PTF alloy can be ascribed to the following reasons: a) The high pressure utilized in PTF during solidification can squeeze the liquid metal into the last solidified zone of casting, therefore decreasing the shrinkage porosities; b) PTF had a comparatively lower filling velocity in the process of mold filling and thus air entrapment can be effectively avoided; c) Liquid penetration for feeding in the PTF alloy was much easier because of its near spherical morphology of the primary α-Al phases, which resulted from the inherent characteristic of semisolid forming[21,22]; d) The abundant liquid fraction of the PMC alloy, which was much higher than that of the PTF alloy, facilitated the augmentation of entrapped gases and shrinkage porosities in the PMC alloy. It is just due to these factors that the PTF alloy shows a much more compact microstructure than the traditional PMC alloy.

3.2 Influence of solution temperature on microstructure

As is widely accepted, solution treatment is a process during which the eutectic phases dissolve into the primary α-Al phase to form a supersaturated α-Al solid solution. Fig.2 presents the SEM images of the PTF-6061 alloy after being solutionized at different temperatures for 3 h. It is clearly seen that the as-fabricated microstructure was composed of nearly spherical primary α phases with an average diameter of ~16.83 μm (Fig.2a), secondarily primary α phases (Fig.2b) and ambient eutectic structures (Fig.2c). Results from the EDS analysis (Fig.2d) along with a previous study about the phase constituents of Al6061[23] corroborated three constituents of α-Al, Mg_2Si and Si in the eutectic phases, which distributed along grain boundaries in bone-like shapes. As the solution temperature rose, the eutectic phases gradually diminished and almost disappeared when the temperature increased to 535ºC (Fig.2e-g). It must be noted that the differences between the primary α phases and the secondarily solidified structures (including both secondarily primary α phases and eutectic structures) were indistinguishable in each state with further elevating the solution temperature over 560ºC (Figs.2h and i). A deeper insight revealed that at the highest solutionization temperature of 585ºC, some spot-like phases with considerably small size can be observed, generally, in the grain boundaries (Fig.3a). EDS analysis showed that this phase was rich in Al, Fe and Si elements (Fig.3b). Combined with the X-ray diffraction pattern from a preliminary study[14], it should be the AlFeSi phase which was highly thermal stable. This phase should exist in the PTF-6061 alloy regardless of solution treatment. But due to its tiny dispersion and the interference of the eutectic phases having similar morphologies during solution treatment (Figs.2e-h), this phase was hard to be distinguished when the solutionization temperature was below 585ºC.

Besides the above-described variation of the eutectic phases, another marked change is the size change of the α-Al grains, as revealed by the OM images in Fig.4a-d. The corresponding statistical results are displayed in Fig.4e. It is clear that the size of the secondarily primary α phases and primary α phases increased rapidly from as-fabricated state (2.15 and 16.83 μm) to 535ºC (4.98 and 25.13 μm), an enhancement of 131.6% and 49.3%, respectively. Nevertheless, the coarsening speed of these two kinds of phases slowed down with increasing the solution temperature over 535ºC. The size of the secondarily primary α phases (5.78 μm at 585ºC) increased by 16.1%, while that of the primary α phases (27.25 μm at 585ºC) only increased by 8.4%.

In an attempt to deeply understand the above depicted grain coarsening behavior in the PTF alloy, the size variation curves were fitted to determine its obeyed function, which is displayed in Fig.5. It reveals that the growth of the two kinds of grains complies with the traditional growth model within 535ºC (Fig.5a)[25]:

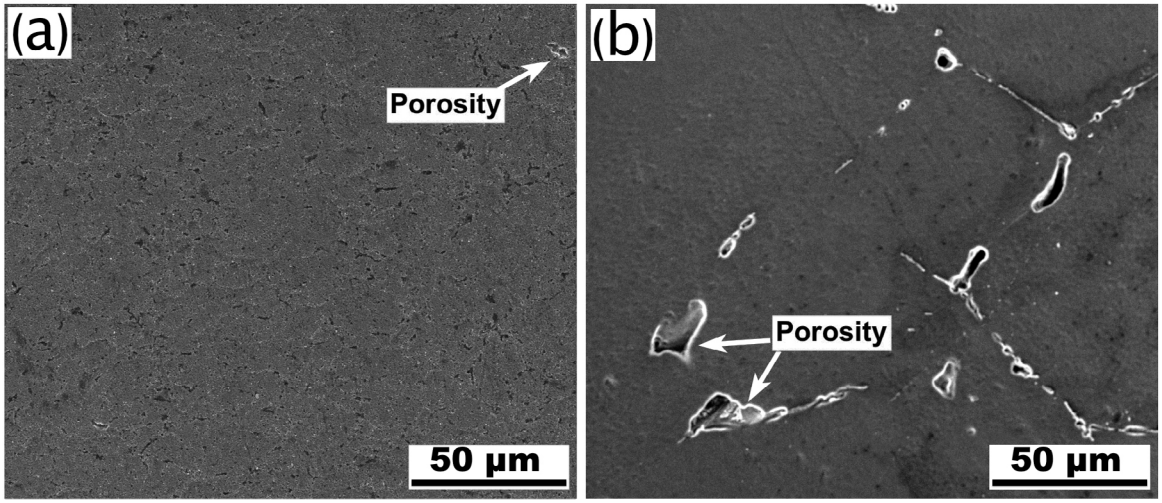

Figure 1. SEM micrographs exhibiting porosity distributions in as-obtained (a) PTF-6061 and (b) PMC-6061 alloys.

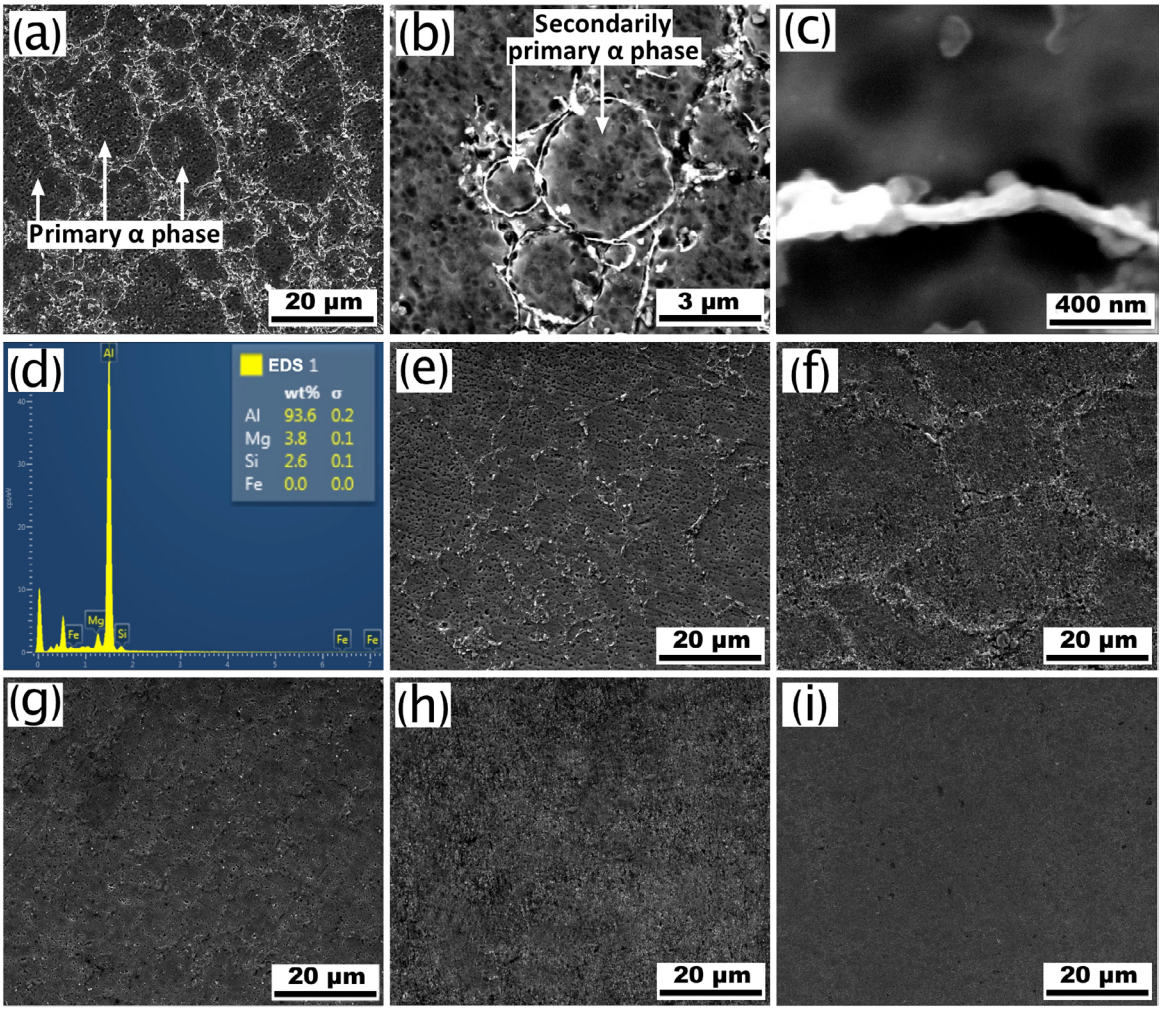

Figure 2. SEM micrographs of the PTF-6061 alloy: (a) as-fabricated state, (b) magnified image showing the details of secondarily primary α phases in (a), (c) magnified image showing the morphology of eutectic phases, (d) EDS analysis of the eutectic phases in (c), and the images of PTF alloy after being solutionized at different temperatures for 3 h: (e) 485ºC, (f) 510ºC, (g) 535ºC, (h) 560ºC and (i) 585ºC.

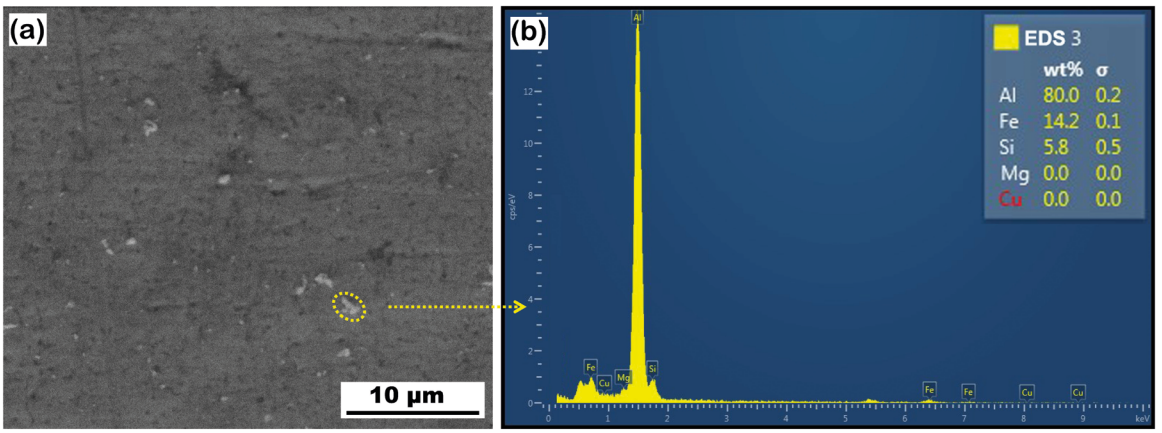

Figure 3. (a) SEM micrograph of the PTF-6061 alloy after being solutionized at 585ºC for 3h, (b) EDS analysis of the circled phase in (a).

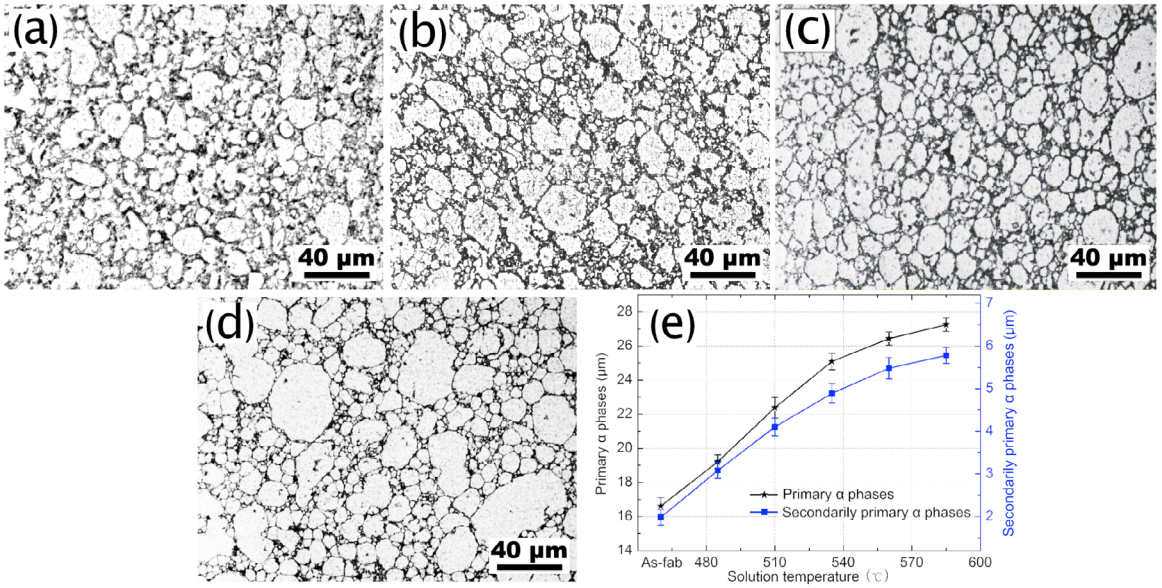

Figure 4. OM images of the PTF-6061 alloy solutionized at various temperatures for 3 h: (a) as-fabricated state, (b) 485ºC, (c) 535ºC, (d) 585ºC and (e) size variations of the primary α phases and secondarily primary α phases as a function of solution temperature (*"As-fab" represents as-fabricated state*).

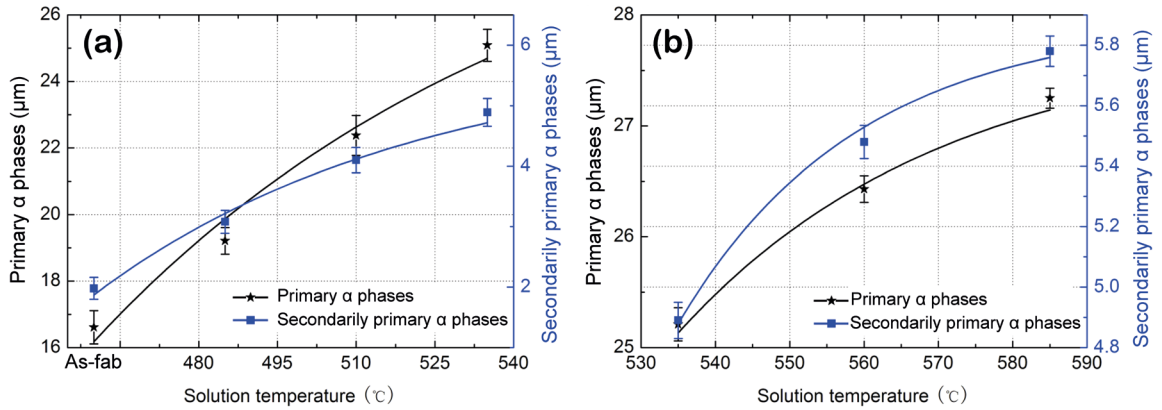

Figure 5. Size variations of the primary α phases and secondarily primary α phases as a function of solution temperature (a) lower and (b) higher than 535ºC.

$$\overline{d} = K(Dt)^n \tag{1}$$

where k represents the growth constant, d is the average grain size, and D stands for the diffusion coefficient that is expressed as:

$$D = D_0 \exp(-Q/RT) \tag{2}$$

where D_0 is the constant of diffusion depended on temperature T, and Q represents the activation energy, which is 160.5 kJ/mol for 6061 aluminum alloy[27]. The obtained results suggest that the n values are 0.87 and 1.23 for the primary α phases and secondarily primary α phases, respectively. It is generally accepted that when n is less than 2, the main motivation for the grain coarsening would be the phase transformation[25]. It can therefore be concluded that the dissolution of eutectic phases plays a dominative role in the growth of these two kinds of grains within 535ºC.

Nevertheless, the growth after 535ºC is distinctly different, and the results shown in Fig.5b indicate that it is subject to the following formula:

$$\bar{d}_t^n - \bar{d}_0^n = kt \tag{3}$$

where $\overline{d}_0$ and $\overline{d}_t$ are the size of initial and final grains, respectively; k and n represent the constants in relation to the interfacial energy, solute concentration and diffusivity; t

is the time, which is equal to the solution temperature in this work because the effect of temperature rising is somewhat identical to that of time elongation on the solutionization progress. The obtained results disclose that the *n* values are 3.48 and 3.72 for the primary α phases and secondarily primary α phases, respectively, which are lower than 4 but larger than 3. In accordance with the existing theory for grain coarsening, *n* will be 4 and 3 respectively if the coarsening is dominated by atom diffusion along the grain boundaries and diffusion through the lattice[27]. Thus, it can be deduced that the coarsening of these two kinds of grains after 535ºC is subject to a mixture model involving atom diffusion along grain boundaries and through the crystal lattice, which lead to interface migration and subsequent grain coarsening. Based on the aforementioned discussion, it is found that the microstructural evolution, particularly the morphology and size changes of α-Al grains, are in good agreement with the dissolution of the eutectic phases in the process of solutionzation.

For reference, the SEM images of the PMC-6061 alloy solutionized at various temperatures for 6 h are displayed in Fig.6. It is found that the as-fabricated microstructure consisted of equiaxed and coarse α dendrites having a mean dimension of ~90.01 μm much larger than that of the PTF alloy and interdendritic net-like eutectic phases, which were distributed along the grain boundaries in large skeleton shapes (Figs.6a and b). Similarly, a certain amount of bright eutectic phases still existed in the alloy at the lowest solutionizing temperature of 485ºC (Fig.6c). The corresponding enlarged views demonstrated that the morphology of the eutectic phases varied from the original large skeleton clusters to the individual spots accompanied with a change in the chemical composition (marked by A in Figs.6c and d). Note that some needle-like phase rich in Al, Fe and Si elements started to appear in the grain boundaries (marked by B in Figs.6c and d) with the gradual dissolution of the eutectic phases. Further elevating the solution temperature to 535ºC, the bright eutectic phases completely disappeared and the needle-like phase with size of 2 to 10 μm can be clearly observed (Fig.6e), which was identified as AlFeSi phase according to the EDS analysis (Fig.6f). This phase is considerably stable in the process of solutionization and cannot dissolve, and its morphology remained nearly unchanged even at the highest solutionization temperature of 585ºC (Figs.6g and h). Simultaneously, it can be observed that the primary grains got coarsened throughout the whole solutionization process.

It is found from the observation above that for the as-fabricated state, the main microstructure differences between PTF and PMC alloys include average grain size, morphology of eutectic phases and the number of pores, as summarized in Table 2. This large discrepancy can be ascribed to the different fabrication methods employed in these two alloys, as displayed in Fig.7. Firstly, the utilization of the "Thixoforming" step in the PTF process could effectively squeeze the liquid metal to the last solidified zone of casting and consequently reduce the shrinkage porosities, thus a significantly decreased amount of pores can be achieved in the PTF alloy; Then, the initial size difference between the "Original powders" (17.91 μm) in PTF process and "Preparation" (bulk alloy) in PMC process leads mainly to the huge grain size discrepancy in the resultant alloys despite the employment of permanent mold with a relatively small diameter (50 mm) to refine grains in the latter process; At last, the differences in the eutectic morphology are the result of the discrepancy in the fabrication methods, such as the different fraction of liquid phase between the "Heating" and "Melting" process, and the different cooling rate between the "Thixoforming" and "Casting" steps, etc. All of these factors account for the large microstructure differences in these two alloys.

During solution treatment, it is observed that the solutionization of the PTF alloy at 535ºC for 3 h can basically dissolve its eutectic phases into α-Al phase, while those in the PMC alloy was not accomplished until being solutionized at 535ºC for 6 h, demonstrating a comparatively slower solutionization progress in the latter alloy. This result can be attributed to the coarser eutectic phases and primary dendrites in the PMC alloy. In this case, a smaller contact area with α-Al phase per unit volume can be achieved and thus a relatively longer time was needed for the PMC alloy to fully dissolve its eutectic phases into α-Al phase under the same solutionization temperature. It can be expected that such a discrepancy in the microstructure evolution of these two kinds materials would result in a difference in their corresponding tensile properties during solution treatment, and the tensile properties of these two materials were detailedly presented in what follows.

3.3 Influence of solution temperature on tensile properties

Fig.8a gives the mechanical properties of the PTF-6061 alloy over solution temperature attained out of the tensile test at room temperature. It is clear that the elongation, ultimate tensile strength (UTS) and yield strength (YS) got rapidly enhanced when the temperature rose to 560ºC. Peak values of 14.5%, 241 MPa and 195 MPa were achieved at 560ºC, an enhancement of 81.3%, 33.9% and 97.0%, respectively, in comparison with the as-fabricated alloy. Further elevating the solution temperature to 585ºC decreased the elongation, UTS and YS to 12.3%, 215 MPa and 187 MPa, respectively.

As is well known, solution treatment is a process during which the eutectic phase dissolve into the α-Al phase. Mg_2Si phase is the main eutectic phase in the 6061 aluminum alloy[24]. The solution treatment gives rise to the dissolution of the Mg_2Si phase into the α-Al phase and therefore the effect of solid solution strengthening is improved, leading to a continuous enhancement of the tensile strengths when the temperature is lower than 560ºC. The elongation increase

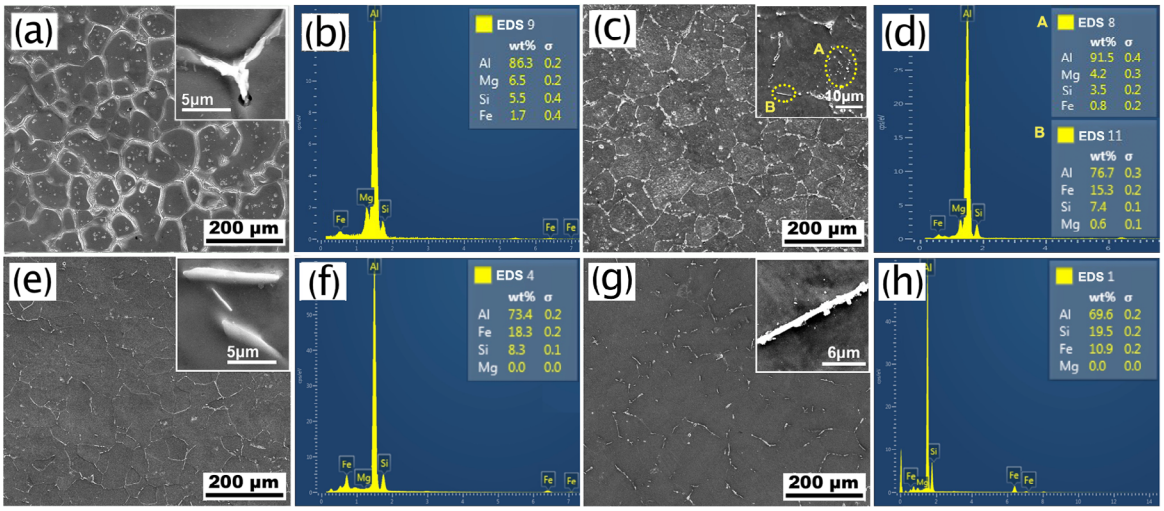

Figure 6. SEM micrographs of the PMC-6061 alloy after being solutionized at various temperatures for 6 h: (a) as-fabricated state, (b) EDS analysis of (a), (c) 485ºC, (d) EDS analysis of (c), (e) 535ºC, (f) EDS analysis of (e), (g) 585ºC, (h) EDS analysis of (g).

Table 2. Summary of the microstructure characteristics of the PTF-6061 and PMC-6061 alloys in the as-fabricated state.

	Pore amount (%)	Average grain size (μm)	Eutectic morphology
PTF-6061 alloy	0.16	~16.83	bone-like shape
PMC-6061 alloy	3.50	~90.01	large skeleton shape

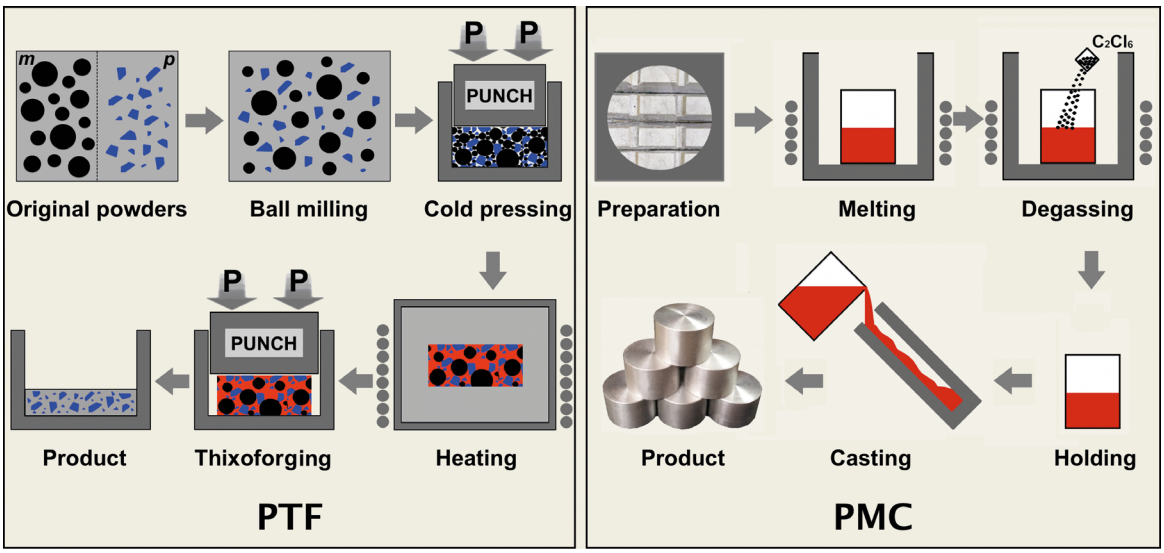

Figure 7. Schematic illustrations of the PTF and PMC process utilized in this work (*m*: matrix; *p*: ceramic particles).

is primarily ascribed to the composition homogenization as well as the enhanced deformation coordination[25]. It must be noted that the effect of solid solution strengthening remains unchanged due to the complete dissolution of Mg_2Si phase at the solutionization temperature of 585ºC and the grains of this alloy are severely coarsened at this time, consequently degrading the tensile properties of PTF alloy to some extent.

For reference, the tensile properties of the PMC-6061 alloy after being solutionized at various temperatures for 6 h are displayed in Fig.8b. Similarly, the PMC alloy firstly showed an increase in the tensile properties (within 560ºC) and then a decrease thereafter. Peak values with an elongation of 24.1%, UTS of 195 MPa and YS of 178 MPa were achieved at 560ºC, which represents an increase of 66.2%, but decreases of 19.1% and 8.7%, respectively, as compared to those of the PTF alloy solutionized at 560ºC for 3 h. The reasons for the variations of the tensile properties were in such a way identical to that for the PTF alloy as stated above.

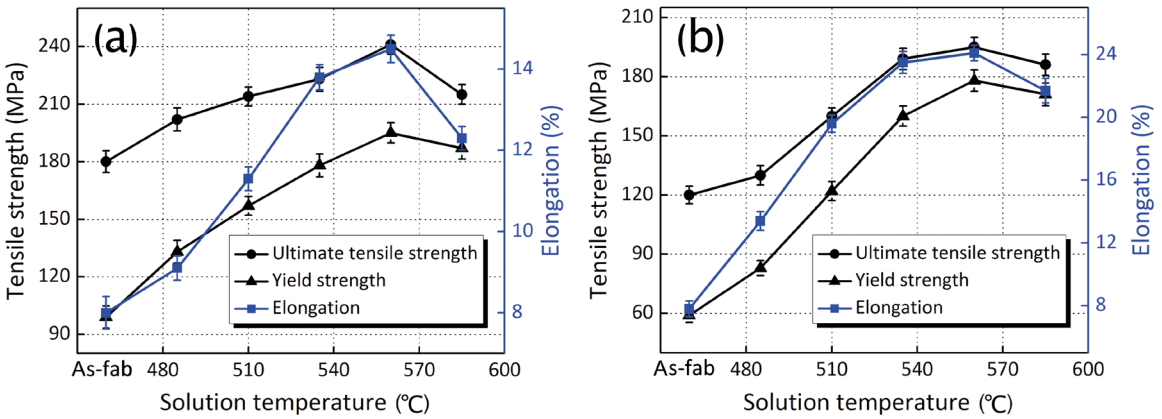

Figure 8. Effects of solution temperature on tensile properties of: (a) PTF-6061 alloy and (b) PMC-6061 alloy.

Based on the above analysis, the superior tensile strengths (including both UTS and YS) of the PTF alloy in comparison with the traditional PMC alloy might result from the following three factors. Firstly, the decreased grain size in the PTF alloy. For instance, the primary grain size of the PMC alloy is ~90.01 μm while that of the PTF alloy is only ~16.83 μm in the as-fabricated state. According to the Hall-Petch equation[26]:

$$\sigma = \sigma_0 + kd^{-1/2} \tag{4}$$

where σ_0 represents the friction stress, k denotes a material constant, d is the average grain size. It is evident that the YS of σ has a reverse relationship with the average grain size. Therefore, finer grain size of the PTF alloy leads to a much higher YS; Second, the enhanced solid solution strengthening due to the much finer eutectic phases in the PTF alloy. For the solutionized alloy, the yield strength difference resulting from the discrepancy in the eutectic phases is mainly achieved through solid solution strengthening. The dissolution of the main solute atoms Mg and Si into the α-Al phases plays an atomic-sized obstacle to prevent dislocations from sliding and thus gives rise to strengthening. The YS increment due to the solid solution strengthening can be calculated by[15]:

$$\Delta\sigma = G\varepsilon(x/4)^{1/2} \tag{5}$$

where G is the shear modulus of the matrix, ε is the fractional difference between the diameters of the solute atoms and the parent atoms, x is the concentration of the solute atoms. This suggests that larger differences between the diameters of the solute and parent atoms as well as the higher atom concentrations result in higher degrees of solid solution strengthening and thus a higher YS. Table 3 shows the atom concentration of elements Mg and Si in the α-Al phases of PTF and PMC alloys with solution temperature, which is determined by EPMA. Clearly, the solute atom concentrations in the PTF alloy are distinctly larger than those of PMC alloy from 485ºC to 535ºC, due likely to the comparatively faster solutionization progress in the PTF alloy. Therefore, the YS contributions from solid solution strengthening are obviously larger than those of PMC alloy within 535ºC. From 560ºC to 585ºC, the atom concentration differences between those two alloys get much smaller, which is in agreement with the relatively smaller YS differences in PTF and PMC alloys at this stage. Finally, the reduced porosities in the PTF alloy. The porosity percentage of the PMC-6061 alloy is up to 3.50% while that of the PTF-6061 alloy is only 0.16%. The higher degree of porosities would act as crack initiations during tensile testing and thus severely degrade the tensile strengths of the PMC alloy. In addition, the insoluble AlFeSi phases in the PTF alloy are found to be significantly smaller than those of PMC alloy. This phenomenon can be more distinctly observed especially after 585ºC (comparing Figs.3a and 6g). These tiny and nearly round phases in the PTF alloy would greatly alleviate local stress concentration around them during tensile testing in comparison with those of the PMC alloy, which are elongated with a large aspect ratio. Thus, the crack initiation sites are greatly reduced and comparatively high tensile strengths can be achieved in the PTF alloy. All of these aforementioned factors contribute to the superior tensile strengths of the PTF alloy than those of the traditional PMC alloy.

The fractographs of the PTF-6061 alloy under different solutionization temperatures were displayed in Figs.9a and b. The fracture surface of the as-fabricated alloy was characterized by small dimples and compact features, no obvious shrinkage porosities as well as other pores can be found (Fig.9a). As is well known, thixoforming was able to reduce or even eliminate porosities and gas pores[14,19,21]. The obtained results revealed that the utilized forming parameters were appropriate to achieve a well feeding ability

Table 3. Atom concentration of elements Mg and Si in the α-Al phases of PTF and PMC alloys determined by EPMA as a function of solution temperature.

Elements	Atom concentration in the α-Al phases (at.%)					
	As-fab	485ºC	510ºC	535ºC	560ºC	585ºC
Mg (PTF)	0.610±0.067	0.624±0.089	0.713±0.113	0.764±0.109	0.813±0.125	0.814±0.108
Si (PTF)	0.307±0.013	0.315±0.015	0.397±0.076	0.427±0.083	0.529±0.099	0.531±0.101
Mg (PMC)	0.565±0.092	0.587±0.102	0.698±0.101	0.726±0.126	0.810±0.123	0.815±0.113
Si (PMC)	0.276±0.038	0.297±0.046	0.354±0.080	0.409±0.098	0.531±0.178	0.534±0.178

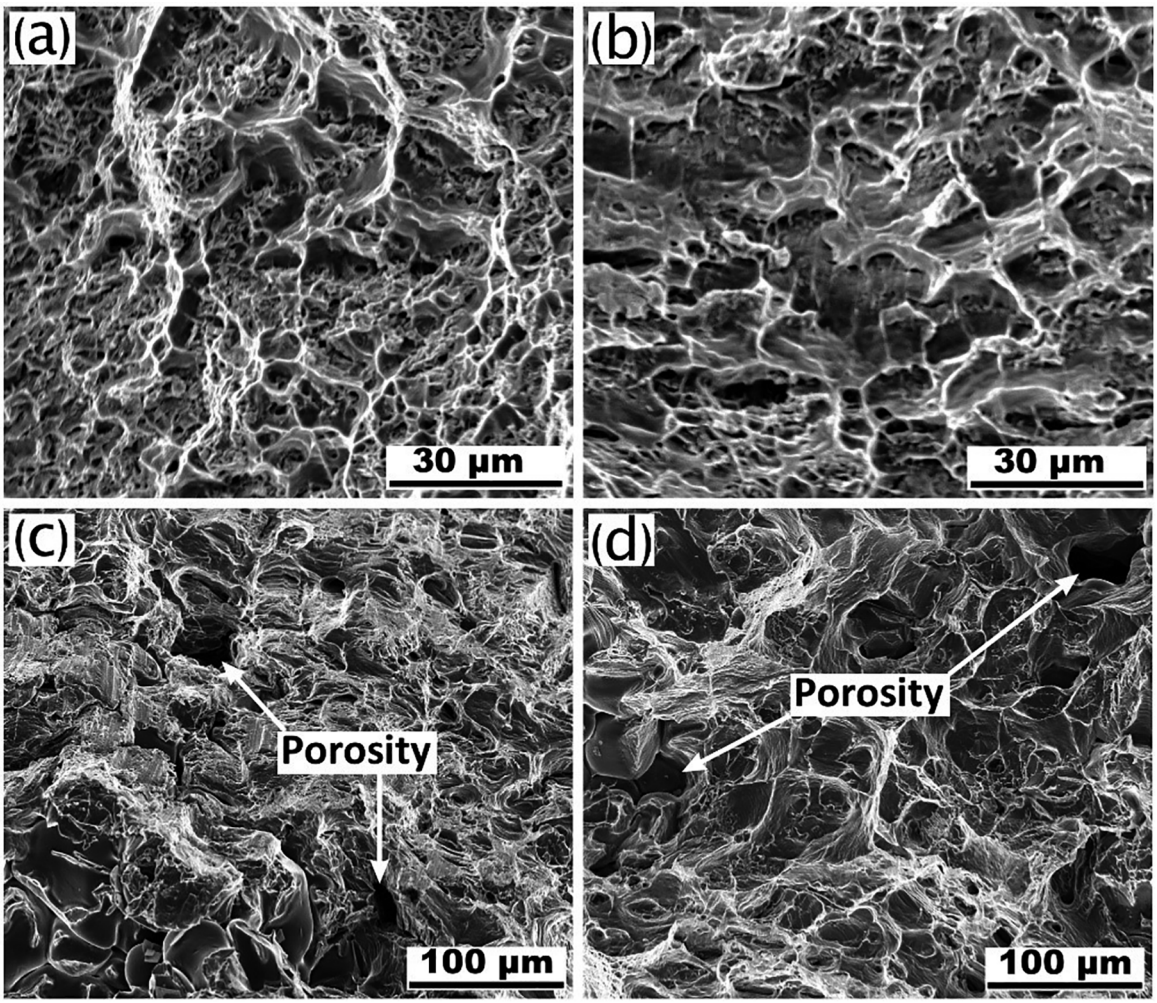

Figure 9. Fractographs of the two kinds of alloys: (a) PTF alloy, as-fabricated state, (b) PTF alloy, solutionized at 560ºC for 3h, (c) PMC alloy, as-fabricated state, (d) PMC alloy, solutionized at 560ºC for 6h.

and mold-filling ability to the solidification shrinkage of the semisolid Al6061 ingot. Hence, applying PTF to fabricate materials with high density was feasible in view of these experimental results in this work. When the PTF alloy was subjected to solution treatment at 560ºC for 3h, lots of flat facets that resulted from cracks propagating across primary α-Al phases appeared (Fig.9b). This indicated that the fracture of PTF alloy may follow a transgranular mode at this time, which was a sign of improved tensile strengths for the thixoformed materials[22,25]. Besides, the amount of the dimples became less but its size was observed to be larger than the as-fabricated state, suggesting an improvement in the elongation of the PTF alloy after solution treatment. In comparison, the fracture surface of as-fabricated PMC alloy was porous and few dimples can be observed, significantly different from that of the PTF alloy (Fig.9c). The porosities

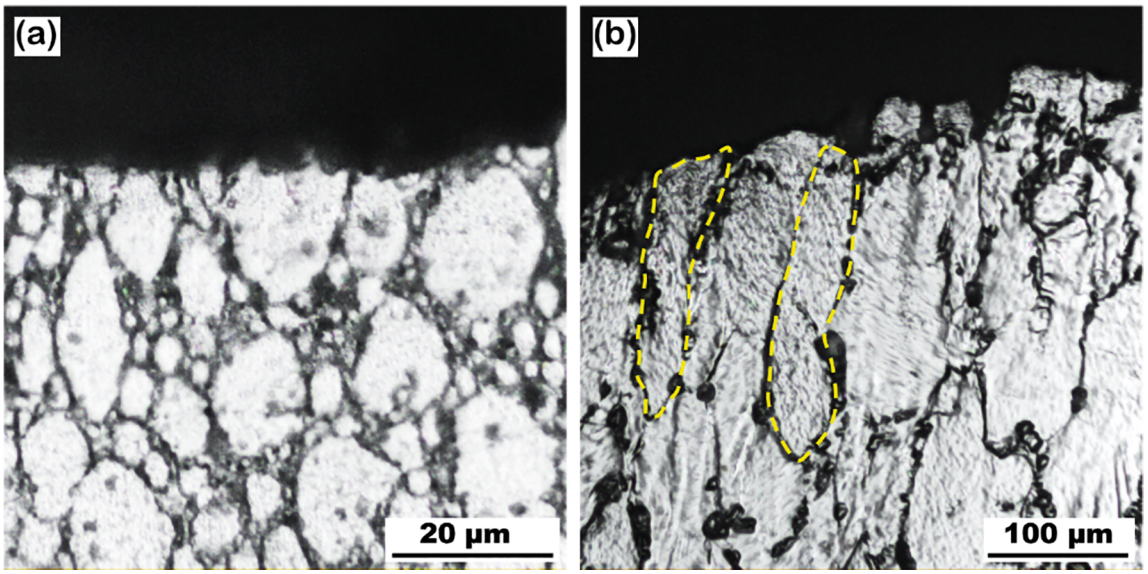

Figure 10. Side view of fracture surfaces of the PTF-6061 alloy (a) and PMC-6061 alloy (b) after being solutionized at 560ºC for 3 and 6h, respectively (*the dot-dashed lines indicate the grain boundaries of the PMC alloy*).

were believed to generate in the last-solidified zones and always harmful to the tensile properties. This corresponded to the relatively lower tensile strengths of the PMC alloy. When the PMC alloy was solutionized at 560ºC for 6h, there were a small quantity of dimples occurring in the fracture surface in addition to the invariant porosities (Fig.9d). This accounted for the improvement in the elongation of the PMC alloy after solution treatment.

It is worthwhile noting that the highest elongation of the PMC alloy after solution treatment (24.1% at 560ºC) was significantly larger than that of the PTF alloy (14.5% at 560ºC). As is well known, tensile elongation is mainly the results of the plastic deformation of grains. Thus, the grains near the fracture surfaces of each alloy were exmained after tensile testing. The results disclosed that the amount of plastic deformation in the PTF particles (Fig.10a) were obviously smaller than that in PMC grains (dot-dashed lines in Fig.10b) during tensile testing. Also, the size of dimples on the fracture surface of the PTF alloy was observed to be relatively smaller (comparing Figs.9b and d), and hence the degree of plastic deformation during tensile testing was less severer than that of the PMC alloy. The reason might be ascribed to the existence of secondarily solidified structures (including secondarily primary α phases and eutectic structures) in the PTF alloy, which always served as weak point in similar alloys[19]. Thus the overall deformation coordination was greatly degraded in this alloy. All of these factors accounted for the superior elongation of the PMC alloy in comparison with the PTF alloy after solution treatment.

4. Conclusions

The following conclusions can be obtained in this work:

1. The pore amount in the PTF-6061 alloy was only 0.16% while that in the PMC-6061 alloy attained 3.50%, the employed PTF technique was effective in decreasing porosities.
2. Solutionization of the PTF alloy at 535ºC for 3 h can basically dissolve its eutectic phases into α-Al phase, while those in the PMC alloy was not accomplished until being solutionized at 535ºC for 6 h. The PTF alloy showed a much quicker solutionization progress than the PMC alloy because of the coarse eutectic phases and primary dendrites in the latter alloy. The insoluble AlFeSi phases in PTF alloy are much rounder and smaller than those in PMC alloy.
3. The dissolution of eutectic phases plays a dominative role in the growth of the primary α phases and secondarily primary α phases within 535ºC. However, the coarsening after 535ºC is subject to a mixture model involving atom diffusion along grain boundaries and through the crystal lattice.
4. With elevating solution temperature, the PTF alloy firstly displayed a significant increase in tensile strengths due mainly to the enhanced solid solution strengthening. Peak values of 14.5%, 241 MPa and 195 MPa in UTS, YS and elongation were achieved at 560ºC, an enhancement of 81.3%, 33.9% and 97.0%, respectively, in comparison with

the as-fabricated alloy. Then a decrease in all of the tensile properties occurred at 585ºC due to the invariant solid solution strengthening and severely coarsened grains.

5. The lower elongation of the PTF alloy than the PMC alloy at the peak condition is the results of poor deformation coordination in the former alloy due to the existence of secondarily solidified structures.
6. The superior tensile strengths of the PTF alloy in comparison with the traditional PMC alloy might result from the decreased grain size, enhanced solid solution strengthening, reduced porosities and the decreased harmful effect of insoluble phases in the PTF alloy.

5. Acknowledgements

The authors wish to express thanks to financial support from the Basic Scientific Fund of Gansu Universities [Grant No. G2014-07]; the Program for New Century Excellent Talents in University of China [Grant No. NCET-10-0023]; and the Program for Hongliu Outstanding Talents of Lanzhou University of Technology [Grant No. 2012-03].

6. References

1. Roy P, Pal TK, Maity J. Transient Liquid Phase Diffusion Bonding of 6061Al-15 wt.% SiC_p Composite Using Mixed Cu-Ag Powder Interlayer. *Journal of Materials Engineering and Performance*. 2016;25(8):3518-3530.

2. Cooke KO. A study of the Effect of Nanosized Particles on Transient Liquid Phase Diffusion Bonding Al6061 Metal-Matrix Composite (MMC) Using Ni/Al_2O_3 Nanocomposite Interlayer. *Metallurgical and Materials Transactions B*. 2012;43(3):627-634.

3. Sajjadi SA, Torabi Parizibi M, Ezatpour HR, Sedghi A. Fabrication of A356 composite reinforced with micro and nano Al_2O_3 particles by a developed compocasting method and study of its properties. *Journal of Alloys and Compounds*. 2012;511(1):226-231.

4. Shamsipour M, Pahlevani Z, Shabani MO, Mazahery A. Optimization of the EMS process parameters in compocasting of high-wear-resistant Al-nano-TiC composites. *Applied Physics A*. 2016;122:457.

5. Rahimian M, Parvin N, Ehsani N. The effect of production parameters on microstructure and wear resistance of powder metallurgy Al-Al_2O_3 composite. *Materials & Design*. 2011;32(2):1031-1038.

6. Wang H, Zhang R, Hu X, Wang CA, Huang Y. Characterization of a powder metallurgy SiC/Cu-Al composite. *Journal of Materials Processing Technology*. 2008;197(1-3):43-48.

7. Sun YP, Yan HG, Chen ZH, Zhang H. Effect of Heat-treatment on Microstructure and Properties of SiC Particulate-Reinforced Aluminum Matrix Composite. *Transactions of Nonferrous Metals Society of China*. 2007;17:S318-S321.

8. Liu P, Wang AQ, Xie J, Hao S. Effect of heat treatment on microstructure and mechanical properties of Si Cp/2024 aluminum matrix composite. *Journal of Wuhan University of Technology*. 2015;30(6):1229-1233.

9. Swamy NRP, Ramesh CS, Chandrashekar T. Effect of heat treatment on strength and abrasive wear behaviour of Al6061-SiCp composites. *Bulletin of Materials Science*. 2010;33(1):49-54.

10. Wang ZG, Li CP, Wang HY, Zhu X, Wu M, Li JH, et al. Aging Behavior of Nano-SiC/2014Al Composite Fabricated by Powder Metallurgy and Hot Extrusion Techniques. *Journal of Materials Science & Technology*. 2016;32(10):1008-1012.

11. Thomas MP, King JE. Comparison of the ageing behaviour of PM 2124 AI alloy and AI-SiC_p metal-matrix composite. *Journal of Materials Science*. 1994;29(20):5272-5278.

12. Dutta I, Allen SM, Hafley JL. Effect of reinforcement on the aging response of cast 6061 Al-Al_2O_3 particulate composites. *Metallurgical & Materials Transactions A*. 1991;22(11):2553-2563.

13. Lai J, Zhang Z, Chen XG. Precipitation strengthening of Al-B4C metal matrix composites alloyed with Sc and Zr. *Journal of Alloys and Compounds*. 2013;552:227-235.

14. Zhang XZ, Chen TJ, Chen YS, Wang YJ, Qin H. Effects of solution treatment on microstructure and mechanical properties of powder thixoforming 6061 aluminum alloy. *Materials Science and Engineering: A*. 2016;662:214-226.

15. Zhang XZ, Chen TJ, Qin YH. Effects of solution treatment on tensile properties and strengthening mechanisms of SiC_p/6061Al composites fabricated by powder thixoforming. *Materials & Design*. 2016;99:182-192.

16. Zhang XZ, Chen TJ. Solution treatment: A route towards enhancing tensile ductility of SiC_p/6061Al composite via powder thixoforming and comparison of micromechanical strength modeling. *Materials Science and Engineering: A*. 2017;696:466-477.

17. Yuan WH, An BL. Effect of heat treatment on microstructure and mechanical property of extruded 7090/SiC_p composite. *Transactions of Nonferrous Metals Society of China*. 2012;22(9):2080-2086.

18. Li G, Zhu DG, Huang QY, Chen GL. Influence of heat treatment on microstructure and properties of Al-Cu alloy prepared by powder metallurgy. *Transactions of Materials and Heat Treatment*. 2011;32(6):63-67.

19. Chen YS, Chen TJ, Zhang SQ, Li PB. Effects of processing parameters on microstructure and mechanical properties of powder-thixoforged 6061 aluminum alloy. *Transactions of Nonferrous Metals Society of China*. 2015;25(3):699-712.

20. Maisonnette D, Suery M, Nelias D, Chaudet P, Epicier T. Effects of heat treatments on the microstructure and mechanical properties of a 6061 aluminum alloy. *Materials Science and Engineering: A*. 2011;528(6):2718-2724.

21. Flemings MC. Solidification processing. *Metallurgical & Materials Transactions A*. 1974;5(10):2121-2134.

22. Zhang SQ, Chen TJ, Cheng FL, Li PB. A Comparative Characterization of the Microstructures and Tensile Properties of as-Cast and Thixoforged *in situ* AM60B-10 vol% Mg_2Si_p Composite and Thixoforged AM60B. *Metals*. 2015;5(1):457-470.

23. Belov NA, Eskin DG, Aksenov AA. *Multicomponent Phase Diagrams: Applications for Commercial Aluminum Alloys*. Oxford: Elsevier; 2005.

24. Zhang HH, Li X, Xiang SQ, Zhou CR, Cai YH. Alloying principle and its application in production of 6××× series wrought aluminum alloy. *Light Alloy Fabrication Technology*. 2012;40(3):12-14.

25. Cheng FL, Chen TJ, Qi YS, Zhang SQ, Yao P. Effects of solution treatment on microstructure and mechanical properties of thixoformed Mg_2Si_p/AM60B composite. *Journal of Alloys and Compounds*. 2015;636:48-60.

26. Tong XC, Ghosh AK. Fabrication of in situ TiC reinforced aluminum matrix composites. *Journal of Materials Science*. 2001;36(16):4059-4069.

27. Huang HJ, Chen TJ, Ma Y, Hao Y. Microstructural evolution during solution treatment of thixoformed AM60B Mg alloy. *Transactions of Nonferrous Metals Society of China*. 2011;21(4):745-753.